Symmetric hybrid surface plasmon polariton waveguides for 3D photonic integration

Yusheng Bian, [1] Zheng Zheng,[1,*] Xin Zhao, [1]Jinsong Zhu,[2] and Tao Zhou[3]

[1] *School of Electronic and Information Engineering, Beihang University, 37 Xueyuan Rd, Beijing 100191, China*
[2] *National Center for Nanoscience and Technology, No.11 Beiyitiao, Zhongguancun, Beijing 100190, China*
[3] *Department of Physics, New Jersey Institute of Technology, Newark, NJ 07102, USA*
**zhengzheng@buaa.edu.cn*

Abstract: A two-dimensional symmetric hybrid plasmonic waveguide that integrates two high-refractive-index dielectric slabs with a finite-width insulator-metal-insulator (IMI) structure is proposed, and the characteristics of its long-range propagation mode are numerically analyzed at 1550 nm wavelength. In contrast to the previously studied structures, the gap between the slabs and the metal stripe and the associated field enhancement effect result in the dramatically modified modal behavior. It is shown that, under optimized configurations, the transmission loss can be reduced significantly with little change in the mode confinement capability compared to similar dielectric-loaded surface plasmon polariton waveguides. Studies on the crosstalk between adjacent such hybrid waveguides reveal the ability to increase the integration density by ~60 times compared with the traditional IMI structures when used in 3D photonic circuits. The studied waveguide could be an interesting alternative to realize high density photonic circuits.

©2009 Optical Society of America

OCIS codes: (240.6680) Surface plasmons; (130.2790) Guided waves; (250.5300) Photonic integrated circuits

References and links

1. W. L. Barnes, A. Dereux, and T. W. Ebbesen, "Surface plasmon subwavelength optics," Nature **424**(6950), 824–830 (2003).
2. S. A. Maier, "Plasmonics: The promise of highly integrated optical devices," IEEE J. Sel. Top. Quantum Electron. **12**(6), 1671–1677 (2006).
3. P. Berini, "Plasmon-polariton waves guided by thin lossy metal films of finite width: Bound modes of symmetric structures," Phys. Rev. B **61**(15), 10484–10503 (2000).
4. J. J. Ju, S. Park, M. S. Kim, J. T. Kim, S. K. Park, Y. J. Park, and M. H. Lee, "Polymer-based long-range surface plasmon polariton waveguides for 10-Gbps optical signal transmission applications," J. Lightwave Technol. **26**(11), 1510–1518 (2008).
5. G. Veronis, and S. H. Fan, "Guided subwavelength plasmonic mode supported by a slot in a thin metal film," Opt. Lett. **30**(24), 3359–3361 (2005).
6. N. N. Feng, M. L. Brongersma, and L. Dal Negro, "Metal-dielectric slot-waveguide structures for the propagation of surface plasmon polaritons at 1.55 μm," IEEE J. Quantum Electron. **43**(6), 479–485 (2007).
7. A. Boltasseva, T. Nikolajsen, K. Leosson, K. Kjaer, M. S. Larsen, and S. I. Bozhevolnyi, "Integrated optical components utilizing long-range surface plasmon polaritons," J. Lightwave Technol. **23**(1), 413–422 (2005).
8. S. Jetté-Charbonneau, R. Charbonneau, N. Lahoud, G. Mattiussi, and P. Berini, "Demonstration of Bragg gratings based on long-ranging surface plasmon polariton waveguides," Opt. Express **13**(12), 4674–4682 (2005).
9. G. S. Wiederhecker, C. M. B. Cordeiro, F. Couny, F. Benabid, S. A. Maier, J. C. Knight, C. H. B. Cruz, and H. L. Fragnito, "Field enhancement within an optical fibre with a subwavelength air core," Nat. Photonics **1**(2), 115–118 (2007).
10. V. R. Almeida, Q. F. Xu, C. A. Barrios, and M. Lipson, "Guiding and confining light in void nanostructure," Opt. Lett. **29**(11), 1209–1211 (2004).
11. R. Zia, M. D. Selker, P. B. Catrysse, and M. L. Brongersma, "Geometries and materials for subwavelength surface plasmon modes," J. Opt. Soc. Am. A **21**(12), 2442–2446 (2004).
12. T. Holmgaard, and S. I. Bozhevolnyi, "Theoretical analysis of dielectric-loaded surface plasmon-polariton waveguides," Phys. Rev. B **75**(24), 245405 (2007).
13. Y. Binfeng, H. Guohua, and C. Yiping, "Bound modes analysis of symmetric dielectric loaded surface plasmon-polariton waveguides," Opt. Express **17**(5), 3610–3618 (2009).

#115253 - $15.00 USD Received 4 Aug 2009; revised 30 Sep 2009; accepted 2 Oct 2009; published 6 Nov 2009
(C) 2009 OSA

14. A. Degiron, C. Dellagiacoma, J. G. McIlhargey, G. Shvets, O. J. F. Martin, and D. R. Smith, "Simulations of hybrid long-range plasmon modes with application to 90° bends," Opt. Lett. **32**(16), 2354–2356 (2007).
15. P. Berini, "Air gaps in metal stripe waveguides supporting long-range surface plasmon polaritons," J. Appl. Phys. **102**(3), 033112 (2007).
16. J. P. Guo, and R. Adato, "Extended long range plasmon waves in finite thickness metal film and layered dielectric materials," Opt. Express **14**(25), 12409–12418 (2006).
17. J. P. Guo, and R. Adato, "Control of 2D plasmon-polariton mode with dielectric nanolayers," Opt. Express **16**(2), 1232–1237 (2008).
18. R. F. Oulton, V. J. Sorger, D. A. Genov, D. F. P. Pile, and X. Zhang, "A hybrid plasmonic waveguide for subwavelength confinement and long-range propagation," Nat. Photonics **2**(8), 496–500 (2008).
19. R. Salvador, A. Martinez, C. Garcia-Meca, R. Ortuno, and J. Marti, "Analysis of Hybrid Dielectric Plasmonic Waveguides," IEEE J. Sel. Top. Quantum Electron. **14**(6), 1496–1501 (2008).
20. R. F. Oulton, G. Bartal, D. F. P. Pile, and X. Zhang, "Confinement and propagation characteristics of subwavelength plasmonic modes," N. J. Phys. **10**(10), 105018 (2008).
21. E. D. Palik, *Handbook of Optical Constants of Solids* (Academic, New York, 1985).
22. E. Prodan, C. Radloff, N. J. Halas, and P. Nordlander, "A hybridization model for the plasmon response of complex nanostructures," Science **302**(5644), 419–422 (2003).
23. R. Buckley, and P. Berini, "Figures of merit for 2D surface plasmon waveguides and application to metal stripes," Opt. Express **15**(19), 12174–12182 (2007).
24. G. Veronis, and S. H. Fan, "Crosstalk between three-dimensional plasmonic slot waveguides," Opt. Express **16**(3), 2129–2140 (2008).

1. Introduction

As a promising candidate to realize ultra-high-density photonic integration and interconnect beyond the diffraction limit, surface plasmon polariton (SPP) waveguides have been intensively studied, due to its potential to confine and guide light at the subwavelength scale [1,2]. While various types of SPP waveguides have been proposed, the insulator-metal-insulator (IMI) [3, 4], and metal-insulator-metal (MIM) waveguides [5, 6] are most widely investigated, and a number of functional devices, such as directional couplers [7], and Bragg gratings [8], had been experimentally demonstrated.

However, in contrast to the promise of achieving the large-scale, high-density integration, the SPP waveguide technology still faces significant challenges when compared with other alternatives, such as photonic crystal waveguides [9], high-contrast dielectric waveguides [10]. The traditional IMI structure can support very low-loss propagation (as low as a few dB/cm) of the long-range SPP mode [4, 7]. However, the low-loss characteristic comes at the expense of poor mode confinement, and its mode size is comparable to that of the conventional dielectric waveguides. On the other hand, the mode in MIM structures is tightly bound in the dielectric slot between the metals and offers truly subwavelength field confinement [5]. Nevertheless, its propagation distance is significantly reduced [6], which renders it less suitable for large-scale integrations. Confining the optical field to the metallic SPP structure and the associated Ohmic loss become a conflict hard to reconcile with [11].

In order to simultaneously realize good propagation length and mode confinement, numerous novel SPP waveguides have been proposed recently. Dielectric-loaded SPP waveguides employing a stripe of high-index dielectric material directly on top of the metal surface are shown to have good lateral and vertical confinement as well as a moderate propagation length [12], and a symmetric dielectric-loaded SPP waveguide with high-index layers placed on both sides of a metal stripe also shows improved performance [13]. A metal stripe buried in a high-index slab can have strong mode guiding capabilities with reduced mode sizes to that of the IMI structure [14]. In contrast, air gaps next to an IMI waveguide are found to be able to lower the loss but easily lead to mode cut-off as well [15]. Covering the metal strip with two thin layers of lower index material can be a better solution to reduce the loss, though the increase in the mode size is still significant [16, 17]. On the other hand, hybrid plasmonic waveguides consisting of a high-index-contrast dielectric waveguide placed very closed to a plasmonic structure have been also proposed [18, 19]. By optimizing the coupling between the dielectric waveguide mode and the SPP mode on a semi-infinite metal-dielectric surface, low-loss, hybrid SPP modes can exist and be strongly confined within the slot between the metal surface and the core of the dielectric waveguide [18, 20].

#115253 - $15.00 USD Received 4 Aug 2009; revised 30 Sep 2009; accepted 2 Oct 2009; published 6 Nov 2009
(C) 2009 OSA

In this paper, the characteristics of a novel symmetric hybrid SPP waveguide based on a traditional long-range SPP waveguide with two high-index structures placed symmetrically near its top and bottom surfaces are investigated. This relatively simple structure, compatible with the photolithography fabrication process, shows the potential to enable subwavelength confinement in the low index gaps between the dielectric slabs and the metal stripe as well as maintaining the long-range propagation characteristics of the traditional IMI waveguides. In contrast to the previous hybrid waveguide [18], the structure studied here possesses finite dimensions in the lateral and vertical directions of its cross section and thus could enable multilayer, 3-dimensional (3D) integrated photonic circuitry. The crosstalk between adjacent hybrid plasmonic waveguides is investigated through simulations as well, and their packing densities are shown to be significantly higher than the traditional IMI waveguides.

2. Geometry and modal properties of the proposed symmetric hybrid SPP waveguide

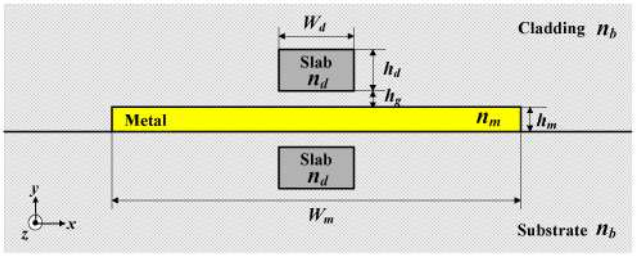

Fig. 1. Schematic diagram of the proposed symmetric hybrid SPP waveguide structure

The cross-section of the proposed symmetric hybrid SPP waveguide, as shown in Fig. 1, consists of a thin metal stripe embedded in a low-index background, and two high-index dielectric slabs located in the substrate and cladding and placed symmetrically near the upper and bottom sides of the metal stripe, respectively. Here the two slabs are assumed to be identical with a rectangular shape of a height h_d and a width W_d. The rectangular shape is considered here for its simplicity and the relative ease to fabricate, while our studies indicate that the following results are also applicable to other kinds of slabs with similar shapes. The edge-to-edge distance between the high-index areas and the metal stripe is denoted as h_g. The width and thickness of the metal stripe are denoted as W_m and h_m, respectively.

In our following simulations, the wavelength λ is set to be 1550 nm. The high-index dielectric material is assumed to be silicon, whose refractive index n_d is taken as 3.478. The substrate and cladding are made of silica with n_b = 1.444. The metal is gold with a refractive index n_m of 0.55+11.5i [21]. In the following sections, without additional explanation, the width and height of the slabs are set at 200 nm and 100 nm [18], respectively, and the gold stripe is 30 nm thick. These parameters are chosen based on the optimization procedures discussed in the following sections. The width of the gold stripe is set to 2 μm, to ensure that the long-range SPP mode studied for comparison still exists under these dimensions. The modal properties are investigated by means of the finite-element method (FEM) using COMSOL^{TM}. The eigenmode solver is used with the scattering boundary condition. Convergence tests are done to ensure that the numerical boundaries and meshing do not interfere with the solutions.

Simulations show that when the dielectric slabs are small and close to the metal stripe, two hybrid bound surface modes can exist through the coupling of the dielectric waveguide mode and the SPP mode [18]. As shown in Fig. 2, we denote the symmetric one as the long-range hybrid SPP mode and the anti-symmetric one as the short-range hybrid SPP mode. The two modes share similarities to the well-known long-range and short-range SPP modes, respectively. However, the existence of the nanometer-size gaps with high index contrast causes strong field enhancement in the gap region. Since the propagation loss of the short-range hybrid SPP mode is nearly 2 orders of magnitude higher than that of the long-range hybrid SPP mode, in the following study, we only focus on the long-range hybrid SPP mode.

#115253 - $15.00 USD Received 4 Aug 2009; revised 30 Sep 2009; accepted 2 Oct 2009; published 6 Nov 2009
(C) 2009 OSA

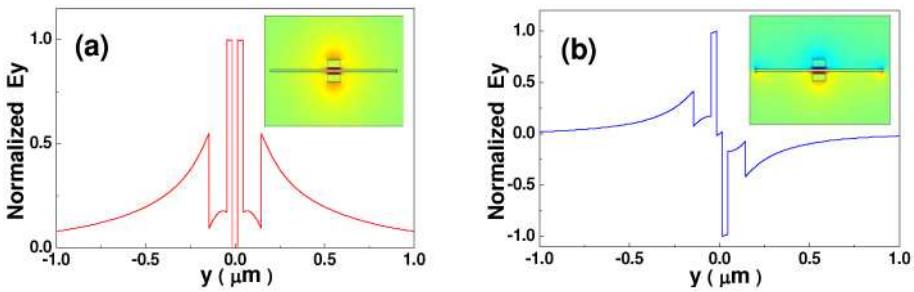

Fig. 2. Normalized Ey distribution along y direction of (a) the long-range hybrid SPP mode; (b) the short-range hybrid SPP mode, where h_g is set at 30 nm.

To further illustrate the effect of the slab and gap on the mode distribution, the energy density distributions of the long-range hybrid SPP mode is compared with that of the modes of a long-range SPP and a symmetric dielectric-loaded SPP waveguide in Fig. 3. The dimensions of the gold stripe in these waveguides are the same, and the sizes and material of dielectric stripes in the symmetric dielectric-loaded SPP waveguide are set to the same as those in the symmetric hybrid SPP waveguide. The results clearly show that, compared to the long-range SPP mode, the long-range hybrid SPP mode is strongly confined around where the slabs are located, and most of the field is concentrated within and near the low refractive index gap, due to the 'slot' effect in the gap [10, 15]. This is in significant difference to that of the symmetric dielectric-loaded SPP mode as well, where the energy is mostly distributed in the high-index dielectric stripes, despite the seemingly similar structures.

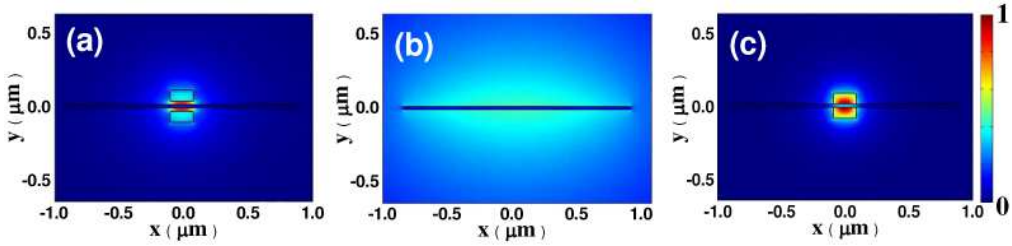

Fig. 3. Energy density distribution of (a) the long-range hybrid SPP mode; (b) the long-range SPP mode; (c) the symmetric mode of the symmetric dielectric-loaded SPP waveguide.

The differences in the key characteristics of these modes are illustrated in Fig. 4, which shows the mode effective index n_{eff} and the propagation length L of long-range hybrid SPP mode when h_g is varied from 2nm to 400nm. The propagation length is given by $L = \lambda/[4\pi/\mathrm{Im}(n_{eff})]$. Similar to the structure discussed in [18], the results indicate that h_g has a remarkable effect on these modal characteristics. When the high-index slabs get closer to the gold stripe, the stronger mode coupling between the long-range SPP mode and the dielectric waveguide mode leads to an increase in n_{eff} and a decrease in L [22]. While the characteristics of the long-range hybrid SPP mode approach those of the symmetric mode of symmetric dielectric-loaded SPP waveguide when the gap diminishes, with a non-zero gap size (between 2 nm and 100 nm), there is a dramatic decrease in n_{eff} and increase in L, indicating a region where both strong field confinement and reduced modal losses can be realized.

A quantitative comparison of the mode confinement is given in Fig. 5, where the normalized energy density distributions and the mode sizes of the above 3 cases are given. h_g is set at 10 nm for the hybrid structure in Fig. 5(a). The mode size is defined as the full width in the dielectric regions where the energy density decays to $1/e^2$ of its peak value [20]. It is obvious that both the lateral and vertical mode sizes of our hybrid mode are more than 1 order of magnitude smaller than those of the long-range SPP mode. It is noted that, due to the non-monotonic distribution of the energy density for the hybrid mode, its calculated mode size in the y direction can be smaller than that of the symmetric mode of symmetric dielectric-loaded

#115253 - $15.00 USD Received 4 Aug 2009; revised 30 Sep 2009; accepted 2 Oct 2009; published 6 Nov 2009
(C) 2009 OSA

SPP waveguide. The figure of merit (FOM) of the hybrid mode, defined as the ratio of L to the effective mode size [17, 23], is found to be between 365 and 646, when the gap height varies from 2 to 100nm. The effective mode size is calculated by the method using the mode sizes in x and y directions [17]. For comparison, the FOM of the symmetric dielectric-loaded SPP mode is 236. The long-range SPP mode has a higher FOM, but it lacks the mode confinement capability of our hybrid mode.

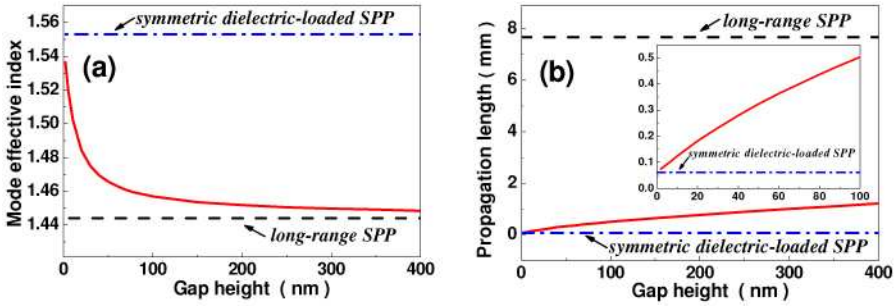

Fig. 4. (a) Mode effective index; (b) Propagation length of the long-range hybrid SPP mode at different h_g.

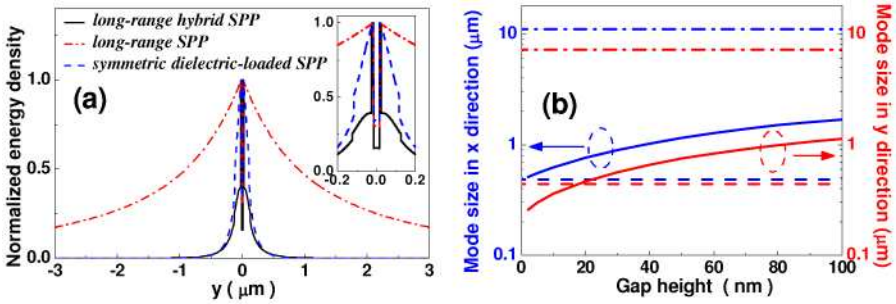

Fig. 5. (a) Profile of the normalized energy density in y direction; (b) Mode sizes at various gap heights. The mode sizes in x and y direction are drawn in blue and red, respectively. Solid line: the long-range hybrid SPP mode, dash-dotted line: the long-range SPP mode, dashed line: the symmetric mode of the symmetric dielectric-loaded SPP waveguide.

The dependence of the waveguide performance on the structure parameters is studied by varying the metal layer thickness and the slab width, respectively. When h_g is fixed at 30nm and the gold thickness is varied from 10nm to 100 nm, it is observed that L increases quickly at the smaller thickness due to the reduced Ohmic loss. Within this range, n_{eff} stays above 1.444 (not shown) even when the thickness is less than 20nm, where the traditional long-range SPP mode will become leaky. As seen in Fig. 6 (b), when the slab width is changed from 100 nm to 1000 nm and h_d is kept at 100nm, the mode size in x direction is shown to decrease first before it increases, which indicates the existence of an optimal width. This can be understood, since the lateral confinement is improved at increased W_d when W_d is relatively small due to the strengthening of the hybrid mode coupling. When the mode is highly confined in the gap, the increase in the slab width proportionally increases the mode size. The propagation length, on the other hand, shows a monotonic decrease at wider slab widths.

3. Crosstalk between adjacent symmetric hybrid SPP waveguides

Crosstalk between adjacent waveguides instead of the physical dimensions of the waveguide dictates the ultimate integration density of the planar photonic circuits [11, 24]. Due to its finite size and planar structure, our proposed hybrid waveguide is suitable for multilayer, 3D photonic circuitry. The crosstalks between two laterally or vertically parallel waveguides are

#115253 - $15.00 USD Received 4 Aug 2009; revised 30 Sep 2009; accepted 2 Oct 2009; published 6 Nov 2009
(C) 2009 OSA

investigated here. The coupling length L_c can be calculated by $L_c = \pi/|k_s - k_a|$, where k_s and k_a are the wavenumbers of the symmetric and anti-symmetric modes of two coupled waveguides, respectively. Figure 7 shows the dependence of the normalized coupling length, i.e. L_c/L, on the center-to-center (CTC) spacing of the waveguides. When L_c/L is larger than 1, the crosstalk would be very small. We can see that both S_x and S_y can be as small as 2.8 μm for the symmetric hybrid SPP (h_g =30nm). In contrast, calculation results show that the S_x and S_y have to be 22 μm for the traditional long-range SPP waveguides to reach L_c/L = 1. Therefore, the proposed hybrid waveguides could potentially improve the overall packing density by nearly 60 times over the traditional IMI structures.

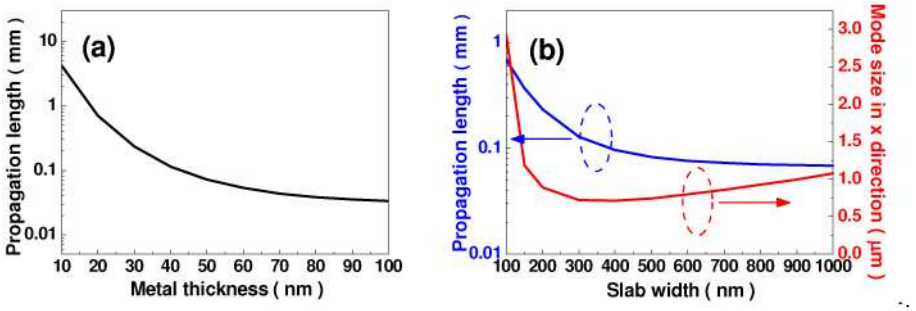

Fig. 6. (a) Propagation length of the hybrid SPP mode at different metal thicknesses; (b) Propagation length and mode size of the hybrid SPP mode at different slab widths.

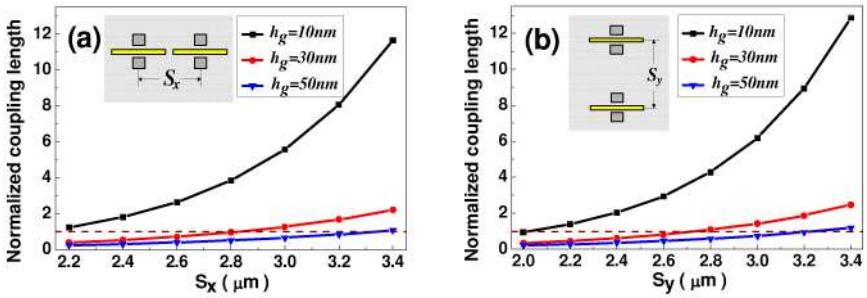

Fig. 7. The dependence of the normalized coupling length on the CTC spacing between two hybrid waveguides. Dash line: L_c/L =1

4. Conclusions

In this paper, we have proposed and studied a symmetric hybrid plasmonic waveguide based on the coupling of two symmetrically placed dielectric slabs and an IMI waveguide. The modal behavior is changed fundamentally by the existence of the high-index-contrast gap between the metal stripe and dielectric slabs. By optimizing the sizes of high-index slabs and the gap, we can achieve both sub-wavelength field confinement and low-loss transmission by increasing the propagation length by several times from that of the symmetric dielectric-loaded SPP waveguide. With an improved field confinement that is 1~2 orders of magnitude higher than that of the long-range SPP structure and a propagation length around hundreds of microns, our symmetric hybrid SPP structure could become an interesting candidate for multilayer sub-wavelength integrated photonic circuits.

Acknowledgements

This work was supported by 973 Program (2009CB930701), NSFC (60877054 / 60921001).

#115253 - $15.00 USD Received 4 Aug 2009; revised 30 Sep 2009; accepted 2 Oct 2009; published 6 Nov 2009

(C) 2009 OSA